

Electroluminescence of ZnO Nanowire/p-GaN Heterojunction Light Emitting Diodes

Xinyu Wang⁺, Jesse Cole⁺, Amir M. Dabiran^{*}, Heiko O Jacobs⁺

⁺Department of Electrical and Computer Engineering, University of Minnesota, Minneapolis, MN 55455

^{*}SVTA Associates, Inc., Eden Prairie, MN 55344

ABSTRACT

This article reports forward and reverse biased emission in vertical ZnO nanowire/p-GaN heterojunction light emitting diodes (LEDs) grown out of solution on Mg-doped p-GaN films. The electroluminescence spectra under forward and reverse bias are distinctly different. Forward bias showed two peaks centered around 390 nm and 585 nm, while reverse bias showed a single peak at 510 nm. Analysis of the current-voltage characteristics and electroluminescence spectra is presented to determine the transport mechanism and location of electron hole recombination. Reverse bias transport and luminescence are attributed to hot-hole injection from the ZnO nanowires into the GaN film through tunneling breakdown. Forward bias transport and luminescence are attributed to hole injection from the GaN into the ZnO and recombination at defect states inside the ZnO yielding distinct color variations between individual wires. Major resistive losses occurred in the GaN lateral thin film connecting to the vertical ZnO nanowires.

Keywords: ZnO, p-GaN, Nanowire, Heterojunction, LED

ZnO is a promising material for exciton-based opto-electronic devices including light emitting (LED) and laser diodes due to its direct band gap of 3.37 eV at room temperature and a large exciton binding energy of 60 meV. Fabrication of LEDs based on ZnO homojunctions, however, has failed due to the lag in production of high quality p-doped ZnO. As a result most work has focused on heterojunction LEDs in particular, polycrystalline n-ZnO thin films grown on single crystal p-GaN substrates [1-4] because of the similar bandgap, small lattice constant mismatch of 1.9%, and identical Wurtzite crystal structure between both materials. While similar, there remains a band offset greater than 1.0 eV which limits injection efficiency at the heterojunction interface[5] to be lower than homojunction devices. More recently the ZnO polycrystalline thin films have been replaced by ZnO nanowires [6, 7] to take advantage of nanowire properties: high crystallinity and fewer grain boundaries when compared with polycrystalline thin films. The results are interesting: One report showed electroluminescence (EL) [6] under reverse bias while the other reported forward bias emission [7].

In this letter, we report on a ZnO nanowire/p-GaN heterojunction LEDs that contrary to previously reported results [6, 7] show EL emissions under both forward and reverse bias. Analysis of the photoluminescence and electroluminescence spectra together with the I-V characteristics suggests different injection mechanisms and locations of electron-hole recombination. Reverse bias results point towards tunneling breakdown where hot carrier injection and recombination predominately occurred in the GaN film. Forward bias emission is attributed to hole injection from the GaN that combine with electrons in the ZnO. The observation of ring shaped EL pattern and distinct colors of individual nanowires will be discussed as well.

The p-GaN templates were prepared by growing a 1- μm thick, highly Mg-doped GaN film on 0.7 μm of resistive GaN grown on a 30 nm thick AlN buffer layer on a c-plane sapphire substrate using RF plasma-assisted molecular beam epitaxy (MBE). The Hall measurements indicated that the hole concentration and mobility of the p-GaN film were $6 \times 10^{17} \text{ cm}^{-3}$ and $9 \text{ cm}^2/\text{V}\cdot\text{s}$, respectively. The resistivity of the film was also measured as 1.2 ohm-cm. The ZnO nanowires were grown on Mg-doped GaN films using a solution method [8]. In brief, ZnO seeds were firstly formed on p-GaN substrate by spinning 1mM zinc acetate in ethanol followed by heat treatment in air at 350 °C for 20 min. The vertically aligned

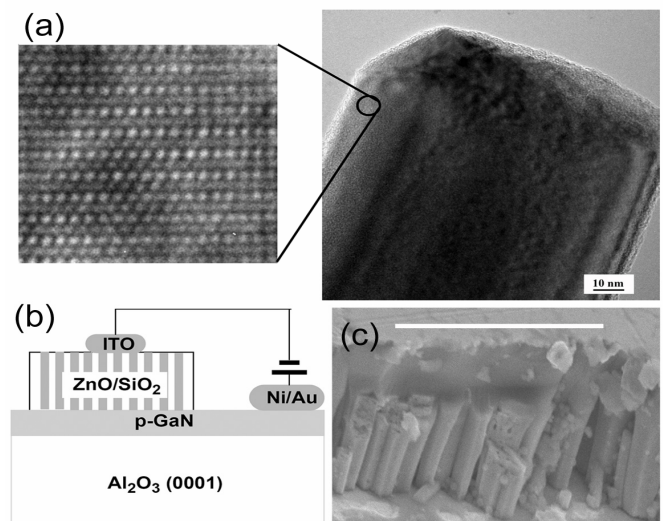


Figure 1: (a) High crystallinity evidenced by high resolution TEM, (b) heterojunction device structure, and (c) SEM image of ZnO nanowire array surrounded by SiO₂ on p-GaN, scale bar: 5 μm

ZnO nanowires were then grown on the seeded p-GaN film in 25 mM aqueous solution of zinc acetate and hexamine at 95 °C for 1 h.

Figure 1 shows a schematic of the device along with a representative TEM and SEM images. The ZnO nanowires were of high crystallinity, as evidenced by XRD and HR-TEM (Fig. 1(a)). The average diameter and length of ZnO nanowires were approximately 80 nm and 1 μm, respectively (Fig. 1c). Figure 1b shows the device structure. To form the illustrated insulating matrix surrounding the ZnO nanowires, we deposited a 1.5 μm thin layer of SiO₂ onto the structure by plasma enhanced chemical vapor deposition (PECVD) at 340 °C at a deposition rate as 40 nm/min, followed by tripod polishing and plasma etching to expose ZnO tips. A portion of the GaN film was masked using photoresist during this process to reserve a window to form a contact to the GaN film. The contact to the GaN was formed using DC sputtered Ni (30nm) followed by Au (100 nm) and rapid thermal annealing in H₂(10%)/N₂(90%) at 500 °C for 30 seconds. For contacts to ZnO nanowires, we RF-sputtered a transparent layer of indium tin oxide (ITO) through a shadow mask, defining a pad diameter of 500 μm. Fig. 1(c) represents the SEM image taken at a location of a scratch to reveal the sandwich structure of ZnO between GaN and SiO₂ films prior to polishing.

Figure 2a compares the photoluminescence (PL) spectra of the isolated materials with the electroluminescence spectra of the fabricated device at room temperature. The PL spectrum of ZnO nanowires (silicon wafer as substrate) consists of an intense near-band-edge UV emission centered at 383 nm and a broad defect-related yellow band with much lower intensity near $\lambda_{\text{max}} \sim 575$ nm. The ZnO near-band-edge emission is attributed to the radiative annihilation of free and bound excitons[9]. In contrast, the PL spectrum of isolated GaN:Mg film consists of an intense near-band-edge band with λ_{max} at 370 nm and a broad band with λ_{max} at 505 nm, which is generally observed in Mg-doped GaN films and is attributed to a radiative recombination involving Mg acceptors[10]. The EL spectra was recorded using a scanning monochromator and photomultiplier tube attached to an upright microscope to record EL spectra from selected areas with a minimal spot size of 100 μm. Under forward bias, the EL spectrum showed two emission peaks: a UV emission centered at 390 nm and a broad, yellow-reddish emission with a maximum (λ_{max}) at 585 nm. The reverse bias EL exhibited a broad peak centered at 510 nm with a small shoulder in the UV at 380 nm.

The comparison between the EL and PL spectra yields the following observation: The forward bias EL spectrum matches the PL spectrum of the ZnO wires, whereas the reverse bias EL spectrum exhibited peak and shoulder locations that match the PL of the GaN. The location of these peaks suggest that under reverse bias electrons and holes recombined predominantly in the p-GaN film, indicating that the EL mechanism differs from conventional forward-biased LEDs.

Figure 2 (b) and (c) show a top view side-by-side comparison of the actual device at 100 x magnification recorded using a CCD camera without changing the capture settings. The individual dots represent emission of a single or clusters containing ~2-5 wires. The emission is not uniform, forward bias emission occurred primarily in a belt towards the edge of the ITO pad showing a small red shift towards the center of the pad. This effect was less pronounced under reverse bias. The color of the EL under reverse bias was bluish green and more nanowires showed emission towards the inner part of the ITO pad with less variation in color. The formation of the illuminated belt under forward bias is explained as in-plane ohmic losses inside the GaN film resulting in a potential drop towards the center region below the required 3V forward bias threshold. The larger threshold voltage (5V) under reverse bias reduces this effect. The actual lifetime of the device has not been determined, however, no noticeable device degradation has been observed over six months operating the device on average once a week for 10 minutes.

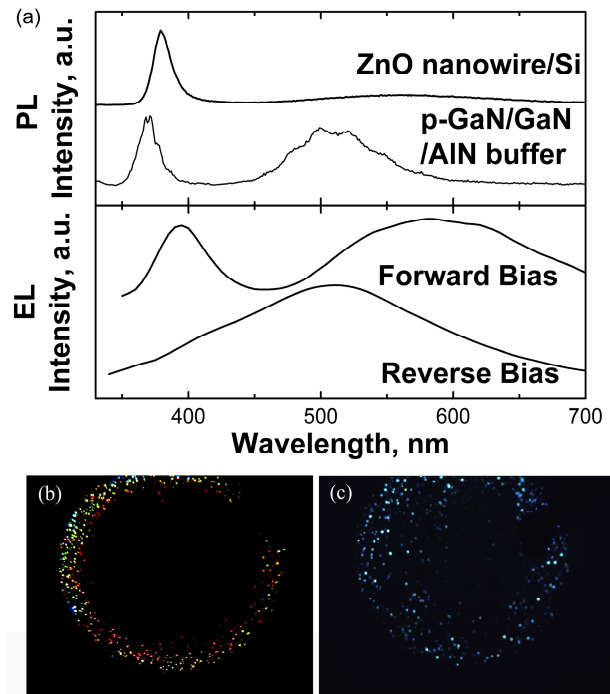


Figure 2: (a) PL spectra of ZnO nanowire arrays and p-GaN film and EL spectra of ZnO nanowire/p-GaN film heterojunction, (b) and (c) top view image (100x) micrograph of EL emission under forward and reverse bias, respectively.

The I-V characteristic of the fabricated ZnO nanowire/p-GaN heterostructure is shown in Fig. 3. A turn on voltage of ~ 3V, leakage current of 1μA, and reverse bias breakdown voltage of 5 V was recorded. The linear portion in the I-V characteristic reveals a large series resistance of 10.8 kΩ. This resistance is caused primarily by the sheet resistance

of p-GaN which was determined to be $12 \times 10^3 \text{ ohm}/\square$ by Hall measurement; the illustrated device used a 5 mm wide contact to the GaN film that was located $\sim 0.7 \text{ mm}$ away from the active area. The influences of the nanowire length and the ITO top contact on the I-V characteristic were insignificant. We doubled the length of the nanowires and did not see a measurable reduction in the current; ITO/ZnO nanowire/ITO test structures showed close to linear I-V characteristics with 50 times smaller differential resistance ($\sim 200 \text{ } \Omega$ per 0.05 cm^2 sized area) suggesting that the ITO/ZnO junction is not dominating the recorded transport. A similar measurement was carried out for the Au-Ni /GaN film/Ni-Au with the same contact layouts. The differential resistance ($\sim 10 \text{ k}\Omega$) is comparable to that of the actual device. Considering these results we suggest that the non-linear diode like portions in the I-V curve of the actual device are caused by the ZnO/GaN heterojunction alone. The insert of Fig. 3 represents the re-plotted I-V curve by subtracting the series resistance of the GaN film. The recorded transport under forward and reverse bias can be explained in terms of band alignment of n-ZnO/p-GaN heterojunction at the interface.

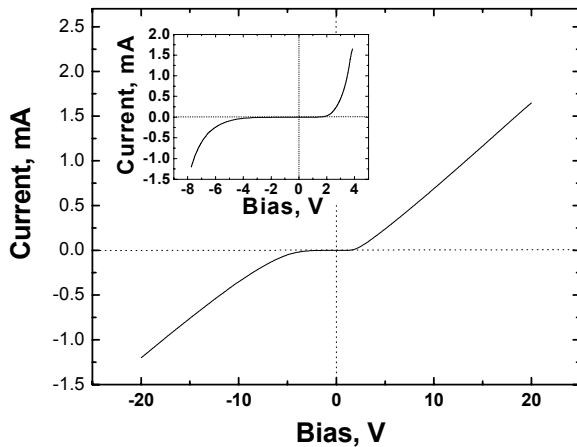


Figure 3: I-V characteristic of ZnO nanowire/p-GaN film heterojunction. Insert: Series resistance corrected I-V.

Under forward bias, holes are expected to be injected from p-GaN into the ZnO nanowires since the energy barrier for holes is less than the barrier for electrons at the heterojunction interface[7]. While this appears to be the case considering the EL spectra we note that the estimated difference in energy barriers (0.13 eV for holes vs. 0.15 eV for electrons) is not significant enough to guarantee injection and recombination exclusively in the ZnO nanowires. Other elements, such as defect states at the ZnO surface and heterojunction interface will play an important role and require further investigation. Another interesting element under forward bias is the variation in the color between individual wires. We cannot explain this variation by quantum size effects or by statistical variation of the number of states and

recombination centers and types inside the wire. Instead we believe that the observed variation is due to different current densities caused by variations in the contact resistance from wire to wire. Wires carrying a high current density due to a reduced contact resistance would involve filling of all states including defect states and near-band-edge states. This explanation is consistent with average emission shifting towards longer wavelength towards the center of the contact where the voltage has dropped due to the in-plane sheet resistance of the GaN film.

As for the EL emission from reverse bias, the mechanism of hole injection and recombination is still under debate. The breakdown mechanism follows the equation derived [11] for tunneling breakdown,

$$J_z = aV^2 \exp\left(-\frac{b}{V}\right)$$

where a and b are constants related to the energy bandgap and doping concentration. The calculated I-V curve shows good agreement for small and medium bias (Figure 4), which is an indication of tunneling breakdown due to the thinning of energy barrier of interface under reverse bias. The actual current begins to exceed the values predicted by tunneling breakdown at high bias suggesting and additional avalanche breakdown component. Pre-breakdown electroluminescence has been reported previously in reversed biased GaN based thin film devices [12]. Accordingly, following a similar argumentation but considering the ZnO nanowire / GaN thin film heterojunction, hot holes are injected from the ZnO conduction band into the GaN valence band and excite electrons from the GaN valence band into the GaN conduction band. Excitation could be enhanced by GaN defects and by confinement of electrons via bandgap differences in the heterojunction.

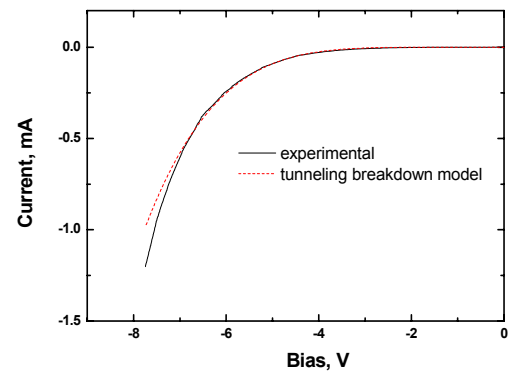


Figure 4: Comparison of the experimental and calculated reverse bias I-V curve considering tunneling breakdown.

In conclusion, ZnO nanowire array/p-GaN film heterojunction diodes were fabricated and their optical and electrical properties were investigated. EL emission emerged under both forward and reverse bias. Contrary to conventional injection under forward bias, tunneling break-down occurred under reverse bias and electron-hole recombination was found to take place in the p-GaN film. In addition, major resistive losses have been identified to occur in the GaN thin film. The reported result should help understand the physics of the operation of ZnO/GaN based heterojunction optoelectronic devices.

This research was directly supported by NSF DMI-0556161 and NSF DMI-0621137. We also acknowledge NSF MRSEC Award DMR-0212302, ECS-0229097, ECS-0407613 for early seed support. We would like to thank Prof. J. Talghader for helpful discussions on device physics and Prof. W. Peria for help and advice on installing a micro-spectrometer.

REFERENCES

- [1] R. D. Vispute, V. Talyansky, S. Choopun, R. P. Sharma, T. Venkatesan, M. He, X. Tang, J. B. Halpern, M. G. Spencer, Y. X. Li, L. G. Salamanca-Riba, A. A. Iliadis, and K. A. Jones, *Applied Physics Letters*, vol. 73, pp. 348-350, 1998.
- [2] Y. I. Alivov, J. E. Van Nostrand, D. C. Look, M. V. Chukichev, and B. M. Ataev, *Applied Physics Letters*, vol. 83, pp. 2943-2945, 2003.
- [3] Y. I. Alivov, E. V. Kalinina, A. E. Cherenkov, D. C. Look, B. M. Ataev, A. K. Omaev, M. V. Chukichev, and D. M. Bagnall, *Applied Physics Letters*, vol. 83, pp. 4719-4721, 2003.
- [4] A. Osinsky, J. W. Dong, M. Z. Kauser, B. Hertog, A. M. Dabiran, P. P. Chow, S. J. Pearton, O. Lopatiuk, and L. Chernyak, *Applied Physics Letters*, vol. 85, pp. 4272-4274, 2004.
- [5] M. W. Wang, J. O. McCaldin, J. F. Swenberg, T. C. McGill, and R. J. Hauenstein, *Applied Physics Letters*, vol. 66, pp. 1974-6, 1995.
- [6] W. I. Park and G.-C. Yi, *Advanced Materials (Weinheim, Germany)*, vol. 16, pp. 87-90, 2004.
- [7] M.-C. Jeong, B.-Y. Oh, M.-H. Ham, and J.-M. Myoung, *Applied Physics Letters*, vol. 88, pp. 202105/1-202105/3, 2006.
- [8] L. E. Greene, M. Law, D. H. Tan, M. Montano, J. Goldberger, G. Somorjai, and P. Yang, *Nano Letters*, vol. 5, pp. 1231-1236, 2005.
- [9] P. Zu, Z. K. Tang, G. K. L. Wong, M. Kawasaki, A. Ohtomo, H. Koinuma, and Y. Segawa, *Solid State Communications*, vol. 103, pp. 459-463, 1997.
- [10] M. A. Khan, Q. Chen, R. A. Skogman, and J. N. Kuznia, *Applied Physics Letters*, vol. 66, pp. 2046-7, 1995.
- [11] R. K. Bhan and V. Gopal, *Semiconductor Science and Technology*, vol. 9, pp. 289-97, 1994.
- [12] D. Starikov, I. Berichev, N. Medelci, E. Kim, Y. Wang, and A. Bensaoula, *AIP Conference Proceedings*, vol. 420, pp. 648-653, 1998.